Simulation of radiated emission by shielded power feeders for electric propulsion of aircraft

Jesper Lansink Rotgerink
Royal Netherlands Aerospace Centre
Marknesse, The Netherlands

***Abstract*—Hybrid electric propulsion as one of the solutions towards sustainable aviation brings on-board a powertrain with high power levels, voltages and currents. In terms of electromagnetic compatibility this will inevitably raise conducted and radiated emission challenges. Power feeders may become a major source of electromagnetic radiation. This paper uses combined multiconductor transmission line and Hertzian Dipole methods to predict such radiated emissions of three-phase power feeders that include shielding. Results of simulated radiated emissions of a shielded trefoil cable are compared to full-wave simulations, models from literature, as well as measured results. Finally, the method is combined with simulated currents in a Simulink model of an electric powertrain, to obtain predicted in-situ radiated emissions of a shielded AC power feeder.**

Keywords—electric flight, radiated emissions, power feeders, multiconductor transmission line, shielding

I. INTRODUCTION

To achieve international climate goals, aviation industry is highly focussed on the development of sustainable aviation. One of the pillars to reach the required 75% reduction in CO_2 emissions per passenger kilometre and 90% reduction in NO_x emissions by 2050 [1], is hybrid electric propulsion. A major challenge in these developments lies in the huge increase of on-board power levels, yielding risks in terms of electromagnetic compatibility. The Horizon 2020 project EASIER (Electric Aircraft System Integration EnableR) is aiming at development of solutions that mitigate these challenges [2].

The significant increase in current and voltage levels, accompanied by high switching frequencies of power electronics, is likely to introduce higher interference currents throughout the electric powertrain. These currents will also flow onto alternate current (AC) power feeders connecting the inverter and motor. In case the power converters will be situated in the pressurized area, these cables can be of significant length, and hence form a considerable source of radiated emissions (RE). Mitigations will have to be found to reduce such radiated emissions to be compliant with EMC standards [3].

Simulation of RE by various power feeder concepts forms a very useful aid in evaluation of various mitigation technologies, as well as system trade-off analyses. A very suitable method of RE prediction from power feeders is given in [4] and [5], in which the Hertzian Dipole (HD) method is used in combination with transmission line (TL) theory. In [4], the HD method is introduced to compute radiated emissions of a single wire or coax above ground, based on the currents on the line. The evolution of these currents over the length of the line is evaluated by known characteristic impedance and fitted load characteristics of the line. In [5] this method, expanded to finite ground plane analysis, is used for prediction of RE of automotive cable bundles following CISPR25 [6]. The paper discusses the estimation of equivalent bundle characteristic impedance and loading, and hence phase evolution of currents, by means of only amplitude measurements.

In [7], multiconductor transmission line (MTL) analysis was combined with the HD method to predict radiated emissions from three-phase power feeders designed for electric propulsion powertrains. The MTL simulations provide phase evolution of the currents over the length of the power feeder, while the magnitude of the currents can be obtained from for instance Matlab Simulink simulation of the entire powertrain. In such a way, in-situ radiated emissions of a power feeder in a complete electric powertrain can be estimated. In this paper, the given methodology will be extended towards three-phase power feeders that include shielding. Obtained results will be cross-compared to simulations with Altair Feko, the methods provided in [4] and [5], as well as measurements.

The following section introduces the MTL and HD method for shielded power feeders. Section III will introduce the measurement set-up used for validation, after which Section IV will discuss results of radiated emission simulations and measurements. Finally, section 0 gives the conclusions.

II. SIMULATION MODEL

Consider the power feeder shown in Fig. 1, which illustrates a trefoil three-phase power feeder with possible shields around each of the phase conductors. MTL modelling can be used to simulate the currents and voltages on each of the conductors, at the cable ends or along the length of the line [8], [9]:

$$\begin{aligned} \frac{d}{dz}\mathbf{V}(z) &= -\mathbf{Z}\mathbf{I}(z) \qquad \mathbf{Z} = \mathbf{R} + \mathrm{j}\omega\mathbf{L} \\ \frac{d}{dz}\mathbf{I}(z) &= -\mathbf{Y}\mathbf{V}(z) \qquad \mathbf{Y} = \mathbf{G} + \mathrm{j}\omega\mathbf{C}. \end{aligned} \tag{1}$$

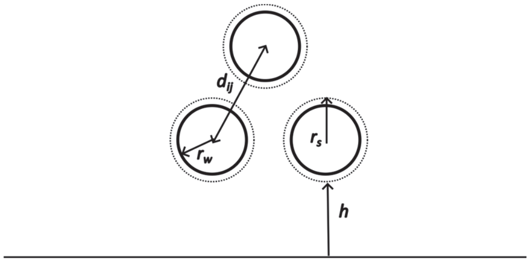

Fig. 1. Cross section sketch of three-phase power feeder above a ground plane. Dashed lines indicate possible shields.

Here ω is the angular frequency, and **V** and **I** are the vectors that contain the voltages with respect to ground and currents of each conductor and z is the propagation direction. The matrices **Z** and **Y** are the per-unit-length (p.u.l.) impedance and admittance matrices, respectively. These can be computed from the p.u.l. resistance matrix **R**, conductance matrix **G**, inductance matrix **L** and capacitance matrix **C**. The conductance includes possible losses in surrounding media, which will be neglected in this paper. Transfer impedance of shielding will be contained in the resistance matrix, in the ways introduced in for instance [9] and [10]. Losses in the phase conductors can also be included in the matrix **R**. The transfer impedance itself is modelled in simplified way for this paper, as a linear combination of transfer resistance R_T and transfer inductance l_T:

$$\begin{aligned} Z_T &= R_T + j\omega l_T \\ R_T &= 3\ \text{m}\Omega/\text{m}, \quad l_T = 0.2\ \text{nH}/\text{m}. \end{aligned} \tag{2}$$

Finally, the inductance and capacitance matrices are derived from analytical expressions for cylindrical conductors, as given in [8]. These matrices contain all geometrical information of the cross section given in Fig. 1. Note that these analytical expressions are subject to some assumptions (e.g. emerged in homogeneous medium, 'wide' separation). Should these be violated, numerical alternatives are present, but these are left out of scope for this paper.

As in [7], the MTL equations in (1) are solved by the chain parameter matrix method. To do so, terminations of the transmission line should be taken into account as boundary conditions. Fig. 2 gives a schematic of the terminations of an electric powertrain taking into account on the source-side the effects of Electromagnetic Interference (EMI) filters, Line Impedance Stabilisation Network (LISN) and output filters, and as load an electric motor [11]. Similarly, Fig. 3 shows the termination schematics representing the set-up for measurement of radiated emissions. In both cases, the transmission line block in the middle handles the evolution of currents and voltages over the length of the line by (1). In both schematics, conductors 1, 3 and 5 are the phase conductors, while conductors 2, 4 and 6 form the corresponding shields. These are grounded at both sides. The infinite ground plane acts as reference conductor. Finally, voltage sources are included on each phase conductor at the source side as excitation of the line. All the effects of the terminations are included into the MTL equations by a Thevenin representation:

$$\mathbf{V}_0 = \mathbf{V}_S - \mathbf{Z}_S \mathbf{I}_0. \tag{3}$$

Here $\mathbf{V}_0$ and $\mathbf{I}_0$ are the vectors containing voltages and currents of each conductor (phase conductors and shields) at the source side of the transmission line. Similarly, these quantities at the load side are represented by $\mathbf{V}_\mathrm{L}$ and $\mathbf{I}_\mathrm{L}$. The voltage sources are contained in the vector $\mathbf{V}_\mathrm{S}$, while the Thevenin equivalent of the termination network at the source side is captured in the source impedance matrix $\mathbf{Z}_\mathrm{S}$. When the three sources are all set to an equal phase, this implies common-mode (CM) excitation, while differential-mode (DM) excitation could be achieved by giving each conductor 120 degrees phase shift. In this paper, focus is on CM excitation.

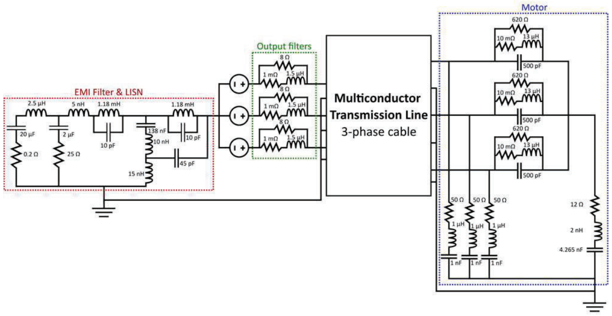

Fig. 2. Terminations of the three-phase shielded power feeder contained in a full powertrain, including at the source side effects of the LISN, EMI filter and output filters, and at the load side the motor.

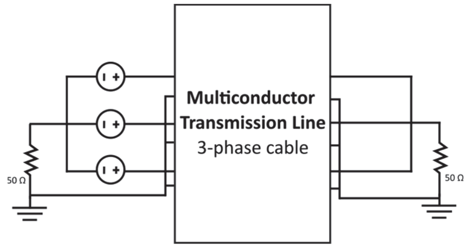

Fig. 3. Terminations of the three-phase shielded power feeder in a measurement set-up.

Making use of the Uniform Cascaded Sections (UCS) method of solving the MTL equations results in currents on all conductors along the entire length of the power feeder. These currents are the cause for radiated emissions, and form input to the HD method. This states that the vertically polarised electric field originating from one segment of a line can be computed by [4][5]:

$$E_v = \frac{I_n \ell z y \eta_0 \beta_0^2}{4\pi r_P^2}\left(\frac{\mathrm{j}}{\beta_0 r_P} + \frac{3}{\beta_0^2 r_P^2} - \frac{3\mathrm{j}}{\beta_0^3 r_P^3}\right)\mathrm{e}^{-\mathrm{j}\beta_0 r_P}. \tag{4}$$

Here the current on each segment is given by I_n, the length of the segment is ℓ, y and z the positions of the observation point with respect to the centre of the segment, β_0 and η_0 the free space propagation speed and intrinsic impedance and finally r_P the distance from segment to observation point. The total field originating from the power feeder is obtained by summation over all cable segments. Similarly to [4], all currents should be mirrored in the infinite ground plane (yielding twice the amount of segments in summation). Moreover, it is very important to include segments from cable end to ground, which carry currents equal to the corresponding ends of the transmission line. For the results in this paper, the longitudinal part of the cable was divided into 1000 segments, while the vertical end wires were divided into 100 segments. In the next sections, the above model will be used to predict radiated emissions from shielded power feeders to both simulations and measurements. The measurement set-up is introduced hereafter.

III. MEASUREMENT SET-UP

Radiated emission measurements were performed to a shielded trefoil sample, manufactured by GKN Fokker Elmo, to perform validation of the simulation models. As was already stated in [7], the set-up used for measurements, as shown in Fig. 4, is based on the procedures of EUROCAE ED-14G [3]. That is, the cables are at 5 cm height and at 10 cm distance from the edge of a conducting table. The length of the test sample after fabrication turned out to be 87 cm, a little shorter than the 1 m dictated by ED-14G. Moreover, ED-14G officially starts at 100 MHz, while test results in this paper start at lower frequencies. Interest in these lower frequencies arises from specific airframers that may still refer back to older ED-14 versions (that did include lower frequency RE), as well as desire to understand behaviour of the powertrain in a broader frequency range (keeping in mind likely integration of more and more on-board sensors in future aircraft). Summarizing, the following frequencies were measured with three different antenna types:

- Rod antenna: 10 kHz – 30 MHz
- Biconical antenna: 30 MHz – 200 MHz
- Double-ridged horn antenna: 200 MHz – 400 MHz

The set-up for the lower frequencies is based on ED-14D, in which the rod antenna set-up is extended with a ground plane attached to the metal table (see Fig. 4a). Finally, only results for the measured and simulated vertical polarised electric field are shown, which are computed and measured at a position consistent with ED-14G, i.e. at 90 cm next to the table and 30 cm above the table. The excitation of the cables is with 10 mA CM currents on all three phase conductors tied together. The excitation is done by a BCI (bulk current injection) method. The cable is directly excited by a Prana power amplifier.

The power feeders are terminated in metallic boxes to prevent radiation from terminal lugs. The shields are properly finished to the termination boxes (see also Fig. 4b). Aluminium foil was used to further minimize leakage from the boxes.

IV. RESULTS

This section details the results of radiated emission simulations by the method introduced in Chapter III. Code-to-code validation of simulation results for a single shielded cable above ground plane is shown in Fig. 4. A cable with length of 1 m, AWG1 inner conductor, and shield with a radius of 5.7 mm, is situated above a perfectly conducting ground plane such that the heart of the inner conductor is at a height of 5 cm (i.e. $h = 4.63$ cm). Terminations are similar to Fig. 3, but then for a single core conductor with single shield (instead of 3 cores and 3 shields). The results shown in Fig. 4 are generated by the method described in the previous section (blue line – referenced as MTL + HD), the full-wave software Feko (red line – due to numerical instabilities for low frequencies only shown for 1.5 MHz and upwards), and the method for radiation from a coax cable as described in [4] (yellow dashed line). The radiated emissions are scaled to an excitation of 1A of the inner conductor over the entire frequency range.

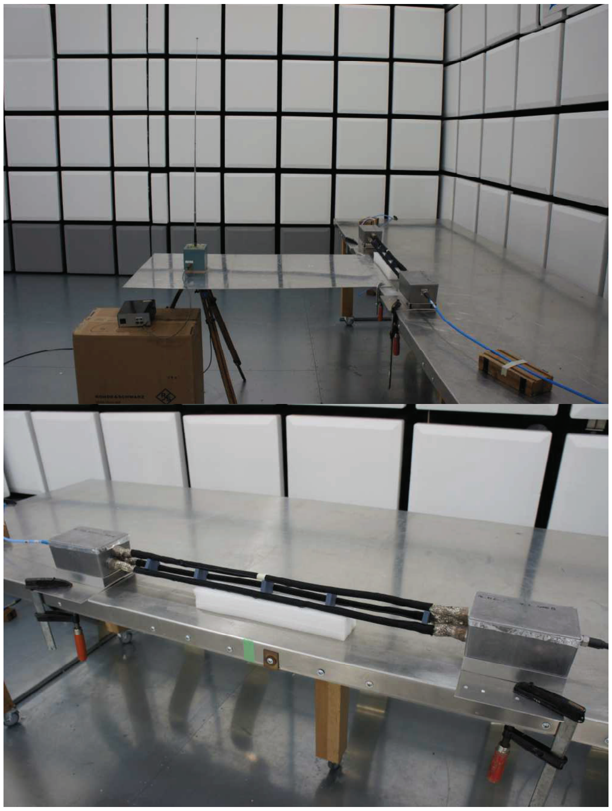

Fig. 4. Pictures of the measurement set-up: a) top picture – with the rod antenna, and b) lower picture –power feeder placed on conducted table.

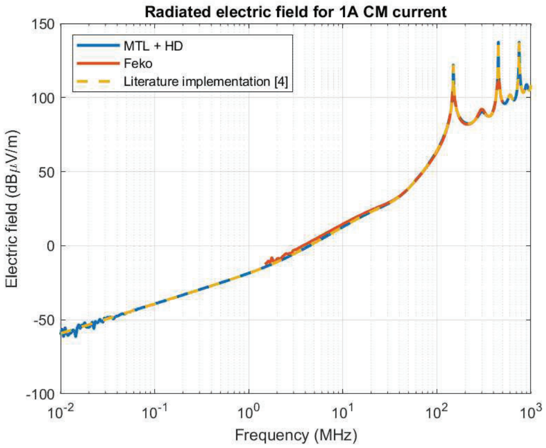

Fig. 5. Code-to-code comparison of simulated radiated emissions for a single coaxial cable.

Clearly, all three methods are in perfect agreement. This is conform expectation, since all methods are ultimately based on transmission line theory.

Fig. 6 shows a comparison between results for simulated and measured radiated emissions of a shielded trefoil power feeder, of which the cross section is shown in Fig. 1. As stated above in section III, the feeder had a length of 87 cm, while the core and shield radius were equal to the previously discussed coax. The height h above ground was 5 cm. Terminations are as given in Fig. 3 and the excitation in this case was a constant 10 mA CM current for all frequencies, applied to all three phase conductors tied together. Simulations with MTL+HD (blue line) are compared to Feko (red line), as well as to measurements (yellow line). The match between MTL+HD and Feko is again very good. Measurements also show a good match with these simulations at the higher frequencies. However, for lower frequencies measured radiated emissions seem to be much higher than the predicted values. For shielded power feeders, the simulated results turn out to be a highly optimized case for which the vertically polarized electric field tends to go to very low values at low frequencies. The currents on the earlier mentioned end connections of the line to ground are very important for proper estimation of radiated emissions. The assumed perfect (and symmetric, i.e. equal at both sides of the line) terminations of the shield in simulations result in the fact that these currents are equal in phase and magnitude at both ends of the line, ensuring radiated emissions that approach very low values at the lowest frequencies. Once an imbalance in the terminations is intentionally introduced (see red line – 10 mΩ bonding on one side of the shield, perfect terminations on the other side) the simulated result is much closer to the measured result. This yields the well-known conclusion that the absolute values of radiated emissions can be highly dependent on the impedances to ground. Hence, it is recommended to carefully analyse the impedances of finishing and interconnects in future research. Nevertheless, even if bonding impedances would contain uncertainties, the model still functions as it should, and trends in radiated emissions for varying parameters should be well predictable.

When applied to an in-situ cable in an electrical propulsion powertrain, of which the terminations are schematically given by Fig. 2, simulated results of radiated emissions are given by Fig. 7 and Fig. 8. Firstly, Fig. 7 shows the radiated emissions as simulated by both Feko and MTL+HD, if the line would be excited by a constant 1A CM current over the full frequency range. This can be considered as transfer function between the amount of current flowing onto the line and the corresponding radiated electric field. The results given by Feko and MTL+HD again match very good. Secondly, to obtain actual levels of radiated emissions that can be expected when the same power feeder is deployed in a powertrain for electric propulsion, this transfer function can be multiplied by either measured or simulated currents in the full powertrain. Fig. 8 shows the radiated emissions if this power feeder would be emerged an actual powertrain. The transfer function in Fig. 7 is therefore scaled by the actual common-mode currents that are simulated in a Simulink model of the entire powertrain [7]. Resulting radiated emissions are compared to limit lines for ED-14G for two different equipment categories. The simulated emissions comply with the category B limit over the full frequency range, and comply for nearly all frequencies with category H.

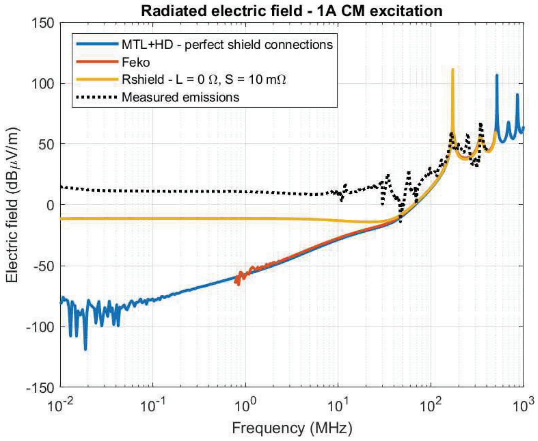

Fig. 6. Comparison of simulated and measured radiated emissions for shielded trefoil power feeder.

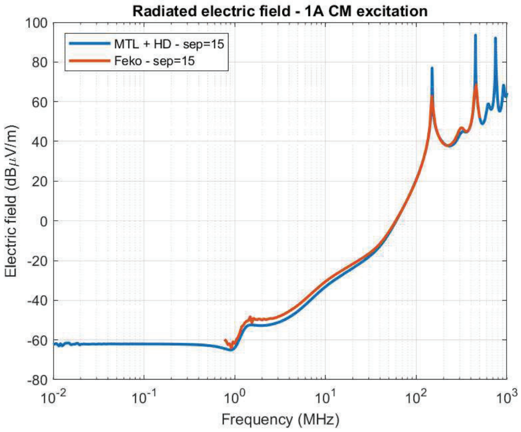

Fig. 7. Simulated radiated electric field when the three-phase power feeder in Fig. 1 is excited by 1A CM currents.

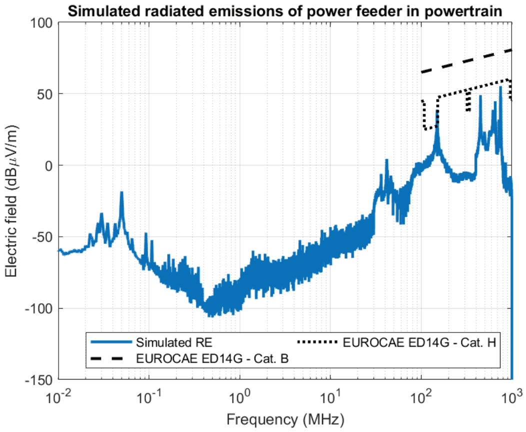

Fig. 8. Simulated total in-situ radiated electric field for a three-phase shielded power feeder in an electric powertrain as given in [7].

ACKNOWLEGDMENT

The EASIER project has received funding from the European Union's Horizon 2020 research and innovation programme under grant agreement No 875504

V. CONCLUSIONS

This paper presented a method to predict radiated emissions from power feeders suitable for use in the evolution of currents over the length of the transmission line, and the latter to convert the currents to electric fields at a given powertrain of (hybrid) electric aircraft. The simulation model combines a multiconductor transmission line and a Hertzian dipole method, in which the first is able to compute the observation point. This paper specifically discusses the radiated emissions resulting from shielded power feeders.

Simulation results with the MTL+HD method of a single coax have been compared to the commercially available Altair Feko and a simulation method from literature. The three results are in perfect agreement. Moreover, predicted radiated emissions from a three-phase shielded power feeder have been compared to both Feko and measurements. Again, the match with Feko is perfect, and also the comparison with measurements at the higher frequencies is good. However, for the lower frequencies, the match with measured emissions highly depends on the applied impedances of the finishing of shields. For perfect terminations, predicted emissions are too perfect (e.g. much lower than measurements). Whenever termination impedances of the shields are introduced, and more specifically an imbalance between the finishing at both sides of the transmission line, measurements and simulations are much more in line. This stresses out the importance of having accurate estimations of the impedances of interconnects and finishing.

Finally, the presented methodology can be used to predict radiated emissions from power feeders emerged in an actual powertrain for electric propulsion. To that extent, a transfer function between currents on the transmission line and radiated electric field, can be combined with actual simulated or measured currents of the power feeder in the powertrain. When done for the case introduced in this paper, comparisons against ED-14G limit lines show that radiated emissions are performing very well. The emissions comply fully with category B limits, and comply for almost all frequencies with category H limits.

REFERENCES

[1] European Commission, "Flightpath 2050: Europe's vision for aviation," LU: Publications office, 2011

[2] EASIER – Electric Aircraft System Integration EnableR, https://www.easier-h2020.eu/

[3] European Organization for Civil Aviation Equipment (EUROCAE), "ED 14, Revision G – Environmental conditions and test procedures for airborne equipment," January 2015.

[4] J. Meng, Y.X. Teo, D.W.P. Thomas, C. Christopoulos, "Fast prediction of transmission line radiated emissions using the Hertzian dipole method and line-end discontinuity methods," IEEE Trans. On Electromagn. Compat., vol. 56, no. 6, Dec. 2014

[5] J. Jia, D. Rinas, S. Frei, "Predicting the radiated emissions of automotive systems according to CISPR 25 using current scan methods," IEEE Trans. On Electromagn. Compat., vol. 58, no. 2, April 2016.

[6] "CISPR 25: Vehicles, boats and internal combustion engines-radio disturbance characteristics – limits and methods of measurements for the protection of on-board receivers," IEC, third ed., 2008.

[7] J. Lansink Rotgerink, "Radiated emissions from power feeders for electric propulsion in aircraft," 2022 International Symposium on Electromagnetic Compatibility (EMC Europe), Gothenburg, Sweden, September 2022.

[8] C.R. Paul, "Analysis of multiconductor transmission lines," New York, NY, USA: Wiley, 1994.

[9] J. Lansink Rotgerink, "Crosstalk Analysis in Aerospace Environments," PhD thesis, University of Twente, Enschede, 2022.

[10] C. Paul, "Transmission-Line Modeling of Shielded Wires for Crosstalk Prediction," IEEE Transactions on Electromagnetic Compatibility, vol. EMC-23, no. 4, pp. 345-351, Nov. 1981.

[11] J. Lee, J. Ha, M. Kim, S. Yun, Y. Kim and W. Nah, "Prediction of Conducted Emission in a PMSM-Drive Braking System Using a Circuit Model Combined with EM Simulation," Intern. Journal of Automotive Techn., vol. 20, pp. 487-498, May 2019.